DETERMINATION OF ACOUSTIC CUT OFF FREQUENCY USING GOLF AND VIRGO INSTRUMENTS

P. Dileep Krishnan[1], Ramkumar Mishra[2]
Department of Physics
Maharishi University of Information Technology (U.P)

ABSTRACT

Graviton-acoustic modes in the Sun and other stars propagate in resonant cavities with a frequency below a given limit known as the cut-off frequency. At higher frequencies, waves are no longer trapped in the stellar interior and become traveller waves. The Global Oscillations at Low Frequency (GOLF) instrument on board *SOHO*) is a resonant scattering spectrophotometer that measures the line-of-sight velocity between the Sun and the spacecraft using the sodium doublet. In this work we have determined the acoustic cutoff frequency of the Sun, *ν*ac, using pseudo mode properties, in particular, the increase in the large separation around *ν*ac that set the limit between *p*-modes and pseudo modes. On the other hand, magnetic activity cycles have begun to be detected in other stars by means of aster seismology Thus, a better knowledge of the behavior of the cutoff frequency would improve our understanding of other stars. By using data gathered by these instruments (GOLF and VIRGO) during the entire lifetime, a variation in the acoustic cutoff frequency with the solar magnetic activity cycle is determined.

Keywords: Sun: helioseismology, GOLF and VIRGO, acoustic cut off frequency

1. INTRODUCTION

Solar *p*-modes are essentially resonant acoustic waves that can be regarded as a superposition of outward and inwardly propagating waves that interfere constructively. At certain discrete frequencies, the interference is maximally constructive, yielding the eigen frequencies of the acoustic cavity within which the *p*-modes propagate. The lower boundary of these resonant cavities lies at a depth inside the Sun at which the horizontal phase speed of the wave equals the local sound speed. The upper boundary of the *p*-mode cavities lies near the solar surface and its location depends on the frequency and wavenumber of the modes. For frequencies higher than a certain value, called the acoustic cutoff frequency (*ν*ac), acoustic disturbances are no longer trapped and propagate as traveling waves through the chromosphere to the base of the corona. Nowadays, it is generally believed that the full-disk-integrated (low-degree) pseudo modes arise from geometric interference between direct waves emitted from a sub photospheric source and indirect waves produced by partial reflection on the far side of the Sun For higher-degree modes, the indirect waves are those emitted downward toward the solar interior and refracted back to the solar surface. The acoustic cutoff frequency is given by $\nu ac = c/2H\rho \propto g/T\text{eff} \propto MR-2T-1/2\text{eff}$, with $H\rho$ being the density scale height, c the sound speed, g the gravitational field, M the mass, R the radius, and Teff the temperature at the photosphere. The acoustic cutoff frequency sets the borderline between *p*-modes and pseudomodes and it is related with other parameters of the oscillation spectrum, for example, *ν*max, the frequency of maximum power of the oscillations. It was conjectured by Brown et al. (1991) that the *ν*max scales the cutoff frequency and the increasing number of observations of solar-like stars has confirmed this relation. *ν*max is associated with the coupling between turbulent convection and oscillations and results from a balance between the damping and the driving of the modes. Aster seismic observations suggest that *ν*max corresponds to the plateau of the damping rates. The intrinsic importance of *ν*ac increases with

asteroseismology because the simple scaling relations for asteroseismic quantities have proven very useful when analyzing stellar oscillations, and these scaling relations use the Sun as a reference. The method of measuring *vac* in this research is as follows. In the acoustic spectrum of the Sun, the large frequencyseparation between consecutive modes of the same degree $\Delta\nu_{n,\_} = \nu_{n,\_} - \nu_{n-1,\_}$ is approximately equal to the inverse of the sound travel time from the upper reflection point to the lower turning point and back. This $\nu_{n,}$ decreases if the lower turning point moves inward (increasing ν or decreasing), or if the outer reflection point moves outward. At a given spherical harmonic, the observed frequency spacing between peaks decreases with increasing frequency. However, several authors have pointed out that, between 5000 and 5500 μHz, the frequency spacing increases slightly, this feature probably being associated with the acoustic cutoff frequency, indicating the transition from trapped to traveling waves. If $\nu_{n,}$ increases around νac, all the peaks with frequencies $\nu > \nu$ac will be shifted relative to the peaks with frequencies $\nu < \nu$ac. Finding the frequency at which these shifts takes place would provide a good measurement of the acoustic cutoff frequency. In the present study, the coherence function between intensity and velocity signals will be used instead of the power spectra to avoid intensity contamination, as will be explained inSection 4. The transition between *p*-modes and pseudomodes also could be observed in other oscillation parameters. In particular, if the phase relations (phase shifts) change for frequencies beyond νac. These phase shifts can correspond to velocity–velocity or intensity–intensity measurements at two different spectral lines (two different formation heights), or to intensity–velocity measurements of spectral lines, narrowband photometry, etc. For velocity–velocity (or intensity–intensity) observations, a phase difference of around 0◦ should be expected in the frequency range corresponding to standing (trapped) waves, For intensity–velocity observations, the phase differences give information about the adiabatic or non-adiabatic behavior of the solar atmosphere. In the adiabatic case, a value of−90◦ or +90◦ (depending on the sign convention for upward/downward positive velocity) is expected for the *p*-mode range and a value of 0◦ for a model close to isothermal For non-adiabatic conditions, the phase differences change with frequency depending on the model used. The results of Jimenez show that in the *p*-mode range the *I*−*V* phase differences do not show an exactly adiabatic behavior but one that is close to it. Our concern in the present investigation is that these *I*−*V* phase differences in the *p*-mode range are found to be close to −90◦, are roughly constant with frequency, and have no dependence on solar activity. The theoretical results of Schmieder show that the *I*−*V* phase differences for frequencies beyond νac also change almost linearly in the frequency range between 5000 and6500 μHz because of the traveling nature of the waves. Taking into account the different *I*−*V* phase relationships between *p*-modes and pseudomodes it would be interesting to know how *I*−*V* phase differences are affected by the transition between standing and traveling waves and determine whether this effect corresponds to νac.

2. INSTRUMENTATION

2.1. VIRGO/SPM (Intensities)

The Solar Photometers (SPM) of the Variability of solar IR radiance and Gravity Oscillations (VIRGO) packageon board the *Solar and Heliospheric Observatory* (*SOHO*) mission, consists of three independentphotometers, centered around 402, 500, and 862 nm(the blue, green, and red channel, respectively). They measure the spatially integrated solar intensity over a 5 nm band pass at a one-minute cadence. The data obtained by the VIRGO/SPM instrumentover the mission have been of uniformly high quality, whether before or after the loss of contact with the spacecraft for several months.

2.2. GOLF (Velocity)

The Global Oscillations at Low Frequency (GOLF) instrument on board *SOHO* is a resonant scattering spectrophotometer that measures the line-of-sight velocitybetween the Sun and the spacecraft using the sodiumdoublet. It uses the same technique as other ground-based helioseismic networks such as the International Research on theInterior of the Sun and the Birmingham Solar Oscillations Network The GOLF window was opened in 1996 January and becamefully operational by the end of that month. Over the followingmonths, occasional malfunctions in its rotating polarizingelements were noticed that led to the decision to stop them

ina predetermined position; truly non-stop observations began by1996 mid-April Since then, GOLF has been continuously and satisfactorily operating in a mode unforeseenbefore launch, showing fewer limitations than anticipated.

Table 1
Time Series Number, Dates, and Sodium Wing Observed by GOLF in Each Period and Mean Duty cycle (DC) of the Time Series Used

Time Series	Dates Interval	Na Wing	DC
0–19	1996 April to 1998 June	Blue	91.7%
20–33	1998 June to 2002 November	Red	99.4%
34–85	2002 November to 2010 May	Blue	97.6%

In Table 1, we summarize the GOLFworking configurations as well as the associated duty cycle of each series.

3. DATA SETS

To study the transition frequency range between *p*-mode sand pseudomodes where *v*ac should be located, the coherenceand phase shift between the intensity and velocity signals willbe used. In phase analyses, the correct timing of the temporalseries is a critical issue that should be carefully addressed. Inthe present case, VIRGO data timing is very well determinedand remained stable throughout the mission. In contrast, GOLFtimings presented some shifts during the mission and required proper correction.

4. DATA ANALYSIS

The method we used to compute the coherence and the phasedifferences is described Briefly, let A and$B$ be two time series of length T and sin$A$, cos$A$, sin$B$, and cos$B$ be the sine and cosine amplitudes of the spectra for series A and B. The power spectral densities, $PA(\nu)$ and $PB(\nu)$, the co spectral density, $CAB(\nu)$, the quadrature spectral density, $qAB(\nu)$,and the complex cross-spectral density, $PAB(\nu)$, are defined as

$$P_A(\nu) = \frac{T}{2}[\sin^2 A(\nu) + \cos^2 A(\nu)]$$

$$P_B(\nu) = \frac{T}{2}[\sin^2 B(\nu) + \cos^2 B(\nu)]$$

$$C_{AB}(\nu) = \frac{T}{2}[\sin A(\nu)\sin B(\nu) + \cos A(\nu)\cos B(\nu)]$$

$$q_{AB}(\nu) = \frac{T}{2}[\sin A(\nu)\cos B(\nu) - \sin B(\nu)\cos A(\nu)]$$

$$P_{AB}(\nu) = C_{AB}(\nu) - iq_{AB}(\nu).$$

The coherence (the analogue of the linear correlation coefficientbetween the two time series A and B in linear regressionanalysis) and the phase difference, $\varphi AB(\nu)$ between series A and B are given by

$$\mathrm{Coh}^2_{AB}(\nu) = \frac{\langle C_{AB}(\nu)\rangle^2 + \langle q_{AB}(\nu)\rangle^2}{\langle P_A(\nu)\rangle\langle P_B(\nu)\rangle} = \frac{|\langle P_{AB}(\nu)\rangle|^2}{\langle P_A(\nu)\rangle\langle P_B(\nu)\rangle}$$

$$\Delta\phi_{AB}(\nu) = \tan^{-1}\left(\frac{\langle q_{AB}(\nu)\rangle}{\langle C_{AB}(\nu)\rangle}\right),$$

The length of the smoothing is not too critical, but needs to be chosen adequately. If it is too short, the parameters are noisy from bin to bin, and if it is too large the frequency resolution is

lost. After several tests varying the length of the smoothing we concluded that five bins is the best tradeoff for this frequency range. The errors for the phase difference are given by

$$\epsilon_{\Delta\phi_{AB}}(\nu) = \sin^{-1}\left(\sqrt{\frac{1-\mathrm{Coh}^2_{AB}(\nu)}{(2n-2)\mathrm{Coh}^2_{AB}(\nu)}}t_{2n-2}\left(\frac{\alpha}{2}\right)\right)$$

Where n represents the equivalent degrees of freedom, $t2n-2(\alpha/2)$ the Student t-distribution, and α the confidence level at which the errors are computed ($\alpha = 0.8$ for phase differences). After computation of the power spectra and vicariate parameters for each pair of four-day time series, these are averaged to obtain four final power spectra (one for each of the three VIRGO/SPM channels and one for GOLF) and three sets of bivariate parameters (coherence and phase shift) between each of the VIRGO/SPM channels with GOLF.

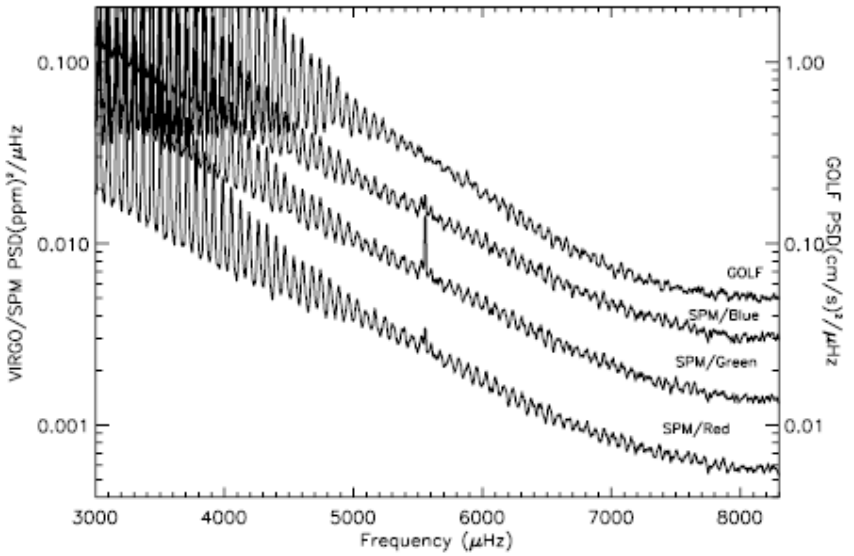

Figure 1. Smoothed power spectra showing the clear periodic structure of pseudomodes for the signals used in this work. Bottom to top: the red, green, and blue channels of VIRGO/SPM and the GOLF spectra.

The VIRGO signals show a peak (highest in the green channel) at just 5555 μHz (see Figure 1) corresponding to three minutes. This is precisely the period of the calibration reference used by the Data Acquisition System of VIRGO. This is an electronic artifact that in principle could contaminate the determination of the acoustic cutoff frequency but, as will be seen in the following sections, it is not a problem because the coherence and phase shift are not affected by this artifact. Indeed, this signal is not present in the GOLF data, and therefore it yields a low value of the coherence at this frequency. The use of power spectra to determine the acoustic cutoff frequency requires special care in the treatment of this instrumental signal, but does not affect the coherence and phase shift on which this work is based.

Figure 2 shows two power spectrum densities, in the range 3000–7000 μHz, (one in intensity and one in velocity). We also show the resultant bivariate parameters. The coherence function has its maxima just where the p-mode maxima lie. This means that the coherence has the relative maxima at the frequencies in which both the intensity and velocity signals are coherent. In the pseudomode range $\nu > 5000$ μHz, the coherence function also shows some maxima because of the presence of pseudomodes in both signals. The visibility of the peaks in the coherence function is much higher than in the power spectra. The bottom plot of Figure 2 shows the phase difference between the intensity and the velocity signals. The exact value of the phase difference is at the frequencies where the coherence function has its maxima, usually close to the maxima of the phase difference function. The phase differences between $I-V$ p-modes are close to the adiabatic value of -90° (see Jim´enez2002), but beyond the acoustic cutoff

frequency ∼5000μHz a change takes place: the phase differences decrease approximately linearly in this region. The frequency at which this different behavior of the phase difference takes place will be studied in Section 6.

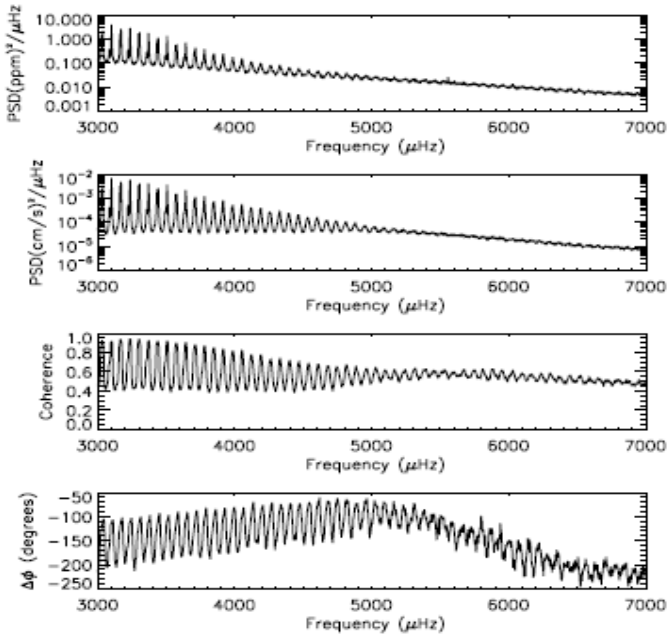

Figure 2. Intensity and velocity power spectra of one of the time series used and the corresponding bivariate parameters between time series, coherence, and phase difference

5. DETERMINATION OF THE ACOUSTIC CUTOFF FREQUENCY

As explained in the Introduction, a change in the valueof the frequency spacing between *p*-modes and pseudomodesis expected because of the increase in the large frequencyseparation around the acoustic cutoff frequency. To find where this frequency spacing change starts to take place, a convenient definition of the acoustic cutoff frequency is derived and adoptedin this section.An exponentially modulated sine wave is fitted to the coherencefunction between 3500 and 5500 μHz to take into accountthe decreasing amplitude of *p*-modes in this frequency range. In Figure 3(a) the coherence function (black line) is plotted between3500 and 6500 μHz, together with the modulated sinewave (blue line) but extended to 6500 μHz. The shape of the solar signal in the pseudomode region(between 5000 and 6500 μHz) is like a sine wave. Thus, a singlesine wave is fitted to the coherence function between 5000 and6500 μHz. This second fit is also plotted in Figure 3(a) (redline) and extended to lower frequencies, down to 3500 μHz. The interval from 5000 μHz to 5500 μHz is used in both fitsbecause it is the interval where the acoustic cutoff frequencyis expected to be found and also because, obviously, it is notpossible to separate *p*-modes from pseudomodes before finding the acoustic cutoff frequency (in several tests this interval has been slightly changed and the same results were obtained).The maxima of the three curves coherence, modulated sine wave, and single sine wave have been computed and plotted inFigure 3(a), where black, blue, and red circles correspond to thefrequencies of the respective maxima of these variables. Up to5000 μHz, the coherence function and the fitted modulated sinewave are in phase and their maxima have the same frequencies.No blue circles are visible below 5000 μHz because they are over plotted by the black ones. Around 5000 μHz, the coherence function starts to shift to higher frequencies and the maxima ofthe fitted modulated sine wave are delayed with respect to those of the coherence function. Blue circles then become visible and the coherence shift increases with frequency, being out of phase (maxima of the coherence coincide with minima of the fitted modulated sine wave) between 6000 and 6500 μHz.

At this point, we define the acoustic cutoff frequency values the crossing point of both frequency differences shown in Figure 3(b). This crossing point is the frequency at which, hypothetically, the maxima of both fitted

functions and the maxima of the coherence coincide.

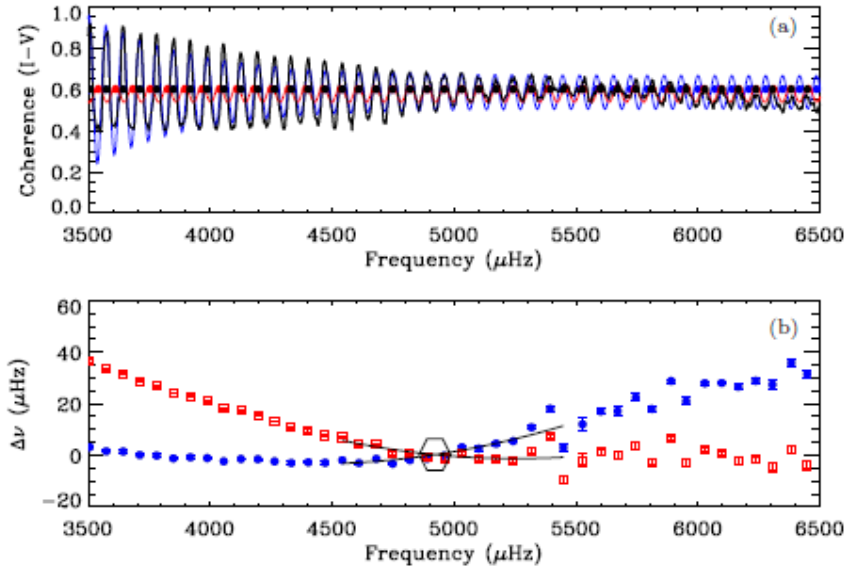

Figure 3. (a) Black line: coherence function. Blue line: exponentially decaying sine wave fitted to the coherence function between 3500 and 5500 μHz (end of the *p*-mode range) and extended to 6500 μHz.

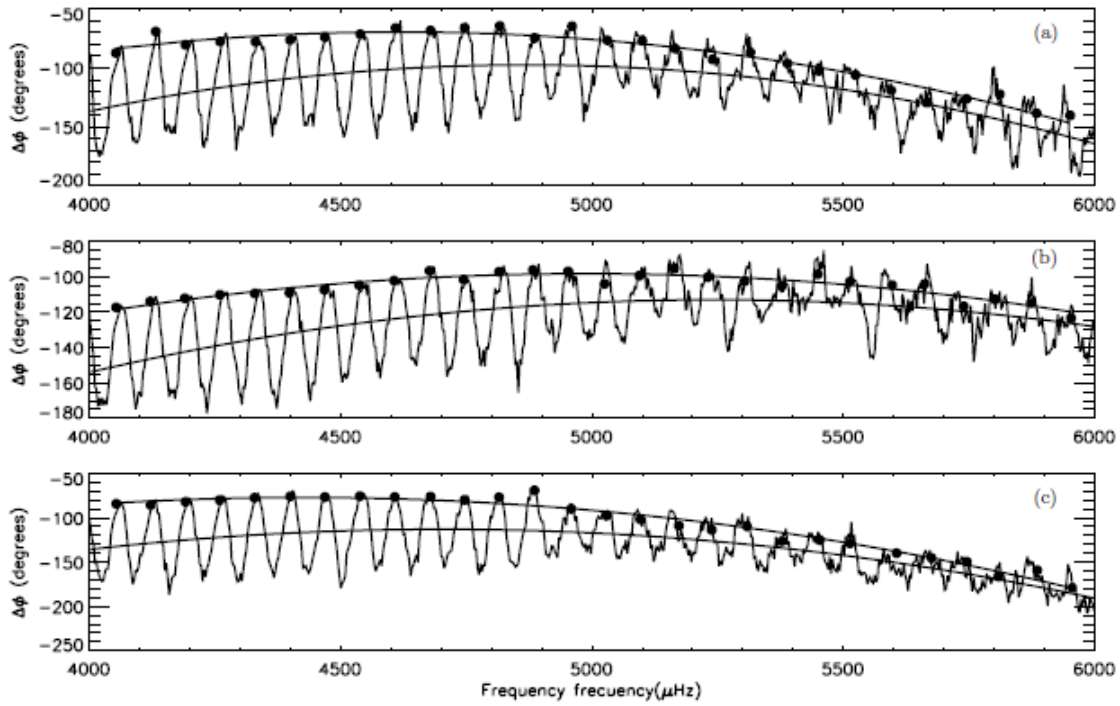

Figure 4 *I*−*V* phase differences in the region 4000 to 6000 μHz for three time series taken at different epochs

Looking around 5000 μHz in Figure 3(b), the blue points arealways below the red ones for lower frequencies and always above for higher frequencies. The frequency interval betweenthe transition of blue points from below to above the red points (indicated by a hexagon) is the frequency interval of the acousticcutoff value. These two limits are the lower and upper limits of *v*ac. A more accurate determination of *v*ac is performed by fitting two parabolas (one for the red points and one for the bluepoints) in the

interval from 4500 to 5500 μHz and computing their crossing frequency point.

6. THE ACOUSTIC CUTOFF FREQUENCY AND THESOLAR ACTIVITY CYCLE

The final values of the acoustic cutoff frequency, computedfrom the 800 day time series described in Section 3, are shown inFigure 5 for the three VIRGO/SPM photometers and for GOLF.The values of the acoustic cutoff obtained as the crossing pointof the two parabolic segments (Figure 3(b)) are represented by black dots whereas the two limits (the frequency intervalbetween the transition of blue points from below to above there d points in Figure 3(b)) are shaded in gray.As mentioned in the Introduction we also investigate howthe $I-V$ phase differences could be affected by the transition between p-modes and pseudomodes. Figure 4shows thephase differences between 4000 and 6000 μHz for three different time series.

7. CONCLUSIONS

In this work we have determined the acoustic cutoff frequency of the Sun, νac, using pseudomode properties, in particular, theincrease in the large separation around νac, that set the limit between p-modes and pseudomodes. Instead of power spectra, we used the coherence function obtained with bivariate analysisbetween simultaneous intensity and velocity time series. Ourresults show that the value of νac is lower than the theoreticalvalue and also lower than previous determinations in whichpower spectra were used without taking into account the influence of the pseudomodes. The exact determination of the solar νac and its variation during the solar cycle is important not only intrinsically, but also for its asteroseismic implications. The dependence of νac with magnetic activity is also verifiedby the position of $I-V$ phase difference maxima in the interval from 4000 μHz to 6000 μHz, indicating transition fromp-modes to pseudomodes. This transition is also correlated withthe solar activity cycle in the same sense but with a hysteresiscycle pattern that could be a manifestation of surface effects ordue to time-delayed responses to a single phenomenon locateddeeper in the Sun.

REFERENCES

[1] Belkacem, K., Goupil, M. J., Dupret, M. A., et al. 2011, A&A, 530, A142
[2] Benomar, O., Baudin, F., Campante, T. L., et al. 2009, A&A, 507, L13
[3] Broomhall, A. M., Chaplin, W. J., Davies, G. R., et al. 2009, MNRAS, 396,L100
[4] Brown, T. M., Gilliland, R. L., Noyes, R.W., & Ramsey, L.W. 1991, ApJ, 368,599
[5] Fossat, E. 1990, Sol. Phys., 133, 1
[6] Fossat, E., Regulo, C., Roca Cortes, T., et al. 1992, A&A, 266, 532
[7] Fr¨ohlich, C., Andersen, B. N., Appourchaux, T., et al. 1997, Sol. Phys., 170, 1
[8] Fr¨ohlich, C., Romero, J., Roth, H., et al. 1995, Sol. Phys., 162, 101
[9] Gabriel, A. H., Charra, J., Grec, G., et al. 1997, Sol. Phys., 175, 207
[10] Gabriel, A. H., Grec, G., Charra, J., et al. 1995, Sol. Phys., 162, 61
[11] Jim´enez, A. 2002, ApJ, 581, 736
[12] Jim´enez, A. 2006, ApJ, 646, 1398
[13] Kumar, P., Fardal, M. A., Jefferies, S. M., et al. 1994, ApJ, 422, L29
[14] Libbrecht, K. G. 1988, ApJ, 334, 510
[15] Marmolino, C., &Severino, G. 1991, A&A, 242, 271
[16] Nigam, R., &Kosovichev, A. G. 1996, Bull. Astron. Soc. India, 24, 195
[17] Pall´e, P. L., Perez, J. C., Regulo, C., Roca Cortes, T., &Isaak, G. R. 1986, A&A,169, 313
[18] Pall´e, P. L., R´egulo, C., Roca Cort´es, T., Sanchez Duarte, L., &Schmider, F. X.1992, A&A, 254, 348
[19] Schmieder, B. 1978, Sol. Phys., 57, 245
[20] Staiger, J. 1987, A&A, 175, 263
[21] Stello, D., Chaplin, W. J., Basu, S., Elsworth, Y., & Bedding, T. R. 2009,MNRAS, 400, L80